The *in vitro* and *in vivo* effects of constitutive light expression on a bioluminescent strain of the mouse enteropathogen *Citrobacter rodentium*

Hannah M. Read[1,2], Grant Mills[1,2], Sarah Johnson[1,2], Peter Tsai[2,3], James Dalton[1,2,4], Lars Barquist[5], Cristin G. Print[2,3,4], Wayne M. Patrick[4,6] and Siouxsie Wiles[1,2,4]

[1] Bioluminescent Superbugs Lab, University of Auckland, Auckland, New Zealand
[2] Department of Molecular Medicine and Pathology, University of Auckland, Auckland, New Zealand
[3] Bioinformatics Institute, School of Biological Sciences, University of Auckland, Auckland, New Zealand
[4] Maurice Wilkins Centre for Molecular Biodiscovery, New Zealand
[5] Institute for Molecular Infection Biology, University of Würzburg, Würzburg, Germany
[6] Department of Biochemistry, University of Otago, Dunedin, New Zealand

ABSTRACT

Bioluminescent reporter genes, such as those from fireflies and bacteria, let researchers use light production as a non-invasive and non-destructive surrogate measure of microbial numbers in a wide variety of environments. As bioluminescence needs microbial metabolites, tagging microorganisms with luciferases means only live metabolically active cells are detected. Despite the wide use of bioluminescent reporter genes, very little is known about the impact of continuous (also called constitutive) light expression on tagged bacteria. We have previously made a bioluminescent strain of *Citrobacter rodentium*, a bacterium which infects laboratory mice in a similar way to how enteropathogenic *Escherichia coli* (EPEC) and enterohaemorrhagic *E. coli* (EHEC) infect humans. In this study, we compared the growth of the bioluminescent *C. rodentium* strain ICC180 with its non-bioluminescent parent (strain ICC169) in a wide variety of environments. To understand more about the metabolic burden of expressing light, we also compared the growth profiles of the two strains under approximately 2,000 different conditions. We found that constitutive light expression in ICC180 was near-neutral in almost every non-toxic environment tested. However, we also found that the non-bioluminescent parent strain has a competitive advantage over ICC180 during infection of adult mice, although this was not enough for ICC180 to be completely outcompeted. In conclusion, our data suggest that constitutive light expression is not metabolically costly to *C. rodentium* and supports the view that bioluminescent versions of microbes can be used as a substitute for their non-bioluminescent parents to study bacterial behaviour in a wide variety of environments.

Subjects Microbiology, Infectious Diseases

Keywords Bioluminescence, *Lux*, Luciferase, Biophotonic imaging, Bioluminescence imaging, Enteric pathogens, Animal model, Reporter genes, Phenotypic microarray, Biolog

Submitted 22 April 2016
Accepted 24 May 2016
Published 22 June 2016

Corresponding author
Siouxsie Wiles,
s.wiles@auckland.ac.nz

Academic editor
Conor O'Byrne

Additional Information and Declarations can be found on page 16

DOI **10.7717/peerj.2130**

INTRODUCTION

Bioluminescence is the by-product of a chemical reaction which has evolved in a wide variety of creatures for different purposes. This 'living light' allows fireflies like *Photinus pyralis* to find a mate (*Vencl*, *2004*), larvae like the New Zealand glow worm *Arachnocampa luminosa* to lure prey (*Meyer-Rochow*, *2007*), and the bacterium *Aliivibrio fischeri* (formally *Vibrio fischeri*) to camouflage its nocturnal symbiont, the Hawaiian bobtail squid, while hunting (*Jones & Nishiguchi*, *2004*). Bioluminescence is produced by the oxidation of a substrate (a luciferin) by an enzyme (a luciferase), which usually requires energy and oxygen. Cloning of the bioluminescence genes from *P. pyralis* (*De Wet et al.*, *1985*), *V. fischeri* (*Engebrecht, Nealson & Silverman*, *1983*) and *Photorhabdus luminescens* (*Szittner & Meighen*, *1990*), has let researchers use light production as a real-time non-invasive and non-destructive surrogate measure of microbial numbers in a wide variety of different culture environments, including within laboratory animals (*Andreu, Zelmer & Wiles*, *2011*). This has proven particularly useful for studying microorganisms which take several weeks to grow on selective media, such as the bacterium *Mycobacterium tuberculosis* (*Andreu et al.*, *2012*; *Andreu et al.*, *2013*). As bioluminescence requires microbial metabolites, such as ATP and reduced flavin mononucleotide ($FMNH_2$), tagging microorganisms with luciferases means only live, metabolically active cells are detected.

Of the available bioluminescent reporter systems, the most widely used in bacteriology research is the bacterial luminescence reaction, encoded by the *lux* gene operon. The reaction involves the oxidation of a long chain aldehyde and $FMNH_2$, resulting in the production of oxidised flavin (FMN), a long chain fatty acid, and the emission of light at 490 nm (*Hastings*, *1978*). The reaction is catalysed by bacterial luciferase, a 77 kDa enzyme made up of an alpha and a beta subunit encoded by the *luxA* and *luxB* genes, respectively. The *luxC*, *D* and *E* genes encode the subunits of a multi-enzyme complex responsible for regenerating the aldehyde substrate from the fatty acid produced by the reaction. A significant advantage of the bacterial bioluminescence system is the ability to express the biosynthetic enzymes for substrate synthesis, allowing light to be produced constitutively. One of the underlying motivations for using *lux*-tagged bacteria is the reduction in the number of animals needed for *in vivo* experiments, an ethical and legislative requirement in many countries. Using a technique known as biophotonic imaging, tagged bacteria can be non-invasively and non-destructively visualised and quantified on multiple occasions from within the same group of infected animals, whereas culture based techniques need groups of animals to be euthanised at each time point of interest (*Andreu, Zelmer & Wiles*, *2011*). However, very little is known about the impact of constitutive light expression on tagged bacteria. We hypothesise that light production will impose a metabolic burden on the tagged bacteria, with the actual fitness costs dependent on the host bacterial species, the site of insertion of the bioluminescence genes and their expression levels.

We have previously made a *lux*-tagged derivative of *Citrobacter rodentium* (*Wiles et al.*, *2005*), a bacterium that infects laboratory mice using the same virulence mechanisms as the life-threatening pathogens, enteropathogenic *Escherichia coli* (EPEC) and entero-haemorrhagic *E. coli* (EHEC) use to infect humans (*Mundy et al.*, *2005*; *Collins et al.*, *2014*).

C. rodentium ICC180 contains a single chromosomally-located copy of the *lux* operon from P. *luminescens*, alongside a gene for resistance to the antibiotic kanamycin. We have previously non-invasively tracked ICC180 during infection of mice (*Wiles et al.*, *2006*), demonstrating that *C. rodentium* rapidly spreads between infected and uninfected animals and that bacteria shed from infected mice are 1,000 times more infectious than laboratory grown bacteria (*Wiles, Dougan & Frankel*, *2005*). While we have shown that ICC180 can reach similar numbers within the gastro-intestinal tracts of infected mice and causes similar pathology when compared to its non-bioluminescent parent strain ICC169 (*Wiles et al.*, *2005*), we have never fully investigated the impact of constitutive light expression on the fitness of ICC180.

In this study we set out to determine whether *C. rodentium* ICC180 has a competitive disadvantage when competed against its non-bioluminescent parent ICC169 in a range of *in vitro* and *in vivo* environments. We also sequenced the genome and associated plasmids of ICC180 to determine whether there were any other genetic differences between the two strains, perhaps as a result of the transposon mutagenesis technique (*Winson et al.*, *1998*) used to generate ICC180. Finally, we compared the growth profiles of the two strains using the BIOLOG Phenotypic Microarray (PM) system, a rapid 96-well microtitre plate assay for phenotypically profiling microorganisms based on their growth under approximately 2,000 different metabolic conditions (*Bochner, Gadzinski & Panomitros*, *2001*).

MATERIALS AND METHODS

Bacterial strains and culture conditions

The bacterial strains used in this study were *Citrobacter rodentium* ICC169 (spontaneous nalidixic acid resistant mutant) (*Wiles et al.*, *2005*) and ICC180 (nalidixic acid and kanamycin resistant) (*Wiles et al.*, *2005*). Bacteria were revived and grown from frozen stocks stored at –80 °C in order to prevent adaptation of *C. rodentium* over multiple laboratory subcultures. Bacteria were grown at 37 °C with shaking at 200 revolutions per minute (RPM) in LB-Lennox media (Fort Richard Laboratories Ltd., Auckland, New Zealand) or in defined minimal media (modified Davis & Mingioli media (*Davis*, *1949*)), containing ammonium sulphate [1 g l^{-1}], potassium dihydrogen phosphate [4.5 g l^{-1}], dipotassium hydrogen phosphate anhydrous [10.5 g l^{-1}], sodium citrate dihydrate [5 g l^{-1}], magnesium sulfate heptahydrate [24.65 mg l^{-1}], thiamine [0.5 mg l^{-1}], supplemented with 1% glucose) at 37 °C. Antibiotics (kanamycin [50 ug ml^{-1}], nalidixic acid [50 ug ml^{-1}]) were only added to the media if they were required for selection. All chemicals and antibiotics were obtained from Sigma-Aldrich (Castle Hill NSW, Australia).

Genome sequencing and analysis

Genomic DNA was prepared from bacteria grown overnight in LB-Lennox broth. Whole genome sequencing was performed using the Illumina HiSeq platform by BGI (Hong Kong). A total of 3,414,820 paired-end 90 bp reads were generated for ICC169 and 3,369,194 for ICC180. Data was quality trimmed using DynamicTrim (*Cox, Peterson & Biggs*, *2010*) (minimum Phred score 25) and filtering of reads shorter than 45 bp after quality trimming was performed using LengthSort (*Cox, Peterson & Biggs*, *2010*); both programmes are part

of the SolexaQA software package (*Cox, Peterson & Biggs*, *2010*). After filtering, 2,444,336 paired reads were retained for ICC169 and 2,383,491 for ICC180. All remaining high quality and properly paired reads were mapped to the reference strain *C. rodentium* ICC168 (Genbank accession number FN543502.1 (*Petty et al.*, *2010*)) using the default settings in BWA (*Li & Durbin*, *2010*). On average, 95% of all high quality reads mapped uniquely to ICC168 (94.8% for ICC169 and 95.2% for ICC180) and single nucleotide polymorphisms (SNPs) and indels that were present only in ICC180 at 100% were identified using Samtools mpileup (*Li et al.*, *2009*). SNPs and indels were confirmed by PCR and sequencing. In addition, the reads were also analysed using BreSeq version 0.24rc6 (*Deatherage & Barrick*, *2014*), which identified predicted mutations that were statistically valid. To locate the insertion site of the lux operon and kanamycin resistance (Km^R) gene, we first performed de novo assembly on quality trimmed data for ICC180 using EDENA v3.0 (*Hernandez et al.*, *2008*). All assembled contigs were mapped to the *C. rodentium* reference strain ICC168 using Geneious (*Kearse et al.*, *2012*) and contigs unmapped to ICC168 were BLAST searched against the *lux* operon and Km^R gene. We located both the *lux* operon and Km^R gene on an unmapped contig 117,921 bp long. To identify the position of this contig, we broke the contig into two segments based on the location of *lux* operon and Km^R gene positions on the contig, and performed additional reference mapping to ICC168 to identify the insertion site. To determine changes to the plasmids present in *C. rodentium*, reads were also mapped to the sequenced plasmids pCROD1 (Genbank accession number FN543503.1), pCROD2 (Genbank accession number FN543504.1), pCROD3 (Genbank accession number FN543505.1), and pCRP3 (Genbank accession number NC_003114).

Phenotypic microarrays

Phenotypic microarrays were performed by BIOLOG Inc. (California, USA) as described previously (*Bochner, Gadzinski & Panomitros*, *2001*). Assays were performed in duplicate using plates PM1-20 (Table S1). The data was exported and analysed in the software package R as previously described (*Reuter et al.*, *2014*). Briefly, growth curves were transformed into Signal Values (SVs) (*Homann et al.*, *2005*) summarising the growth over time while correcting for background signal. Principal component analyses showed a clear separation by genotype, suggesting reproducible differences in metabolism between the two strains. A histogram of log signal values displayed a clear bimodal distribution, which we interpreted as representing non-respiring cells ('off', low SV) and respiring cells ('on', high SV), respectively. Normal distributions were fitted to these two distributions using the R MASS package, and these models were then used to compute log-odds ratios for each well describing the probability that each observation originated from the 'on' or 'off' distribution. Wells which were at least 4 times more likely to come from the 'on' distribution than the 'off' in both replicates were considered to be actively respiring. In order to determine the significance of observed differences between genotypes, we applied the moderated *t*-test implemented in the limma R/Bioconductor package (*Smyth*, *2004*). Wells with a Benjamini–Hochberg corrected *P*-value of less than 0.05, that is allowing for a false discovery rate of 5%, and which were called as actively respiring for at least one genotype, were retained for further analysis. The data was also analysed using the DuctApe software suite (*Galardini et al.*, *2014*). Growth

curves were analysed using the dphenome module, with the background signal subtracted from each well. Based on the results of an elbow test (Fig. S1), 7 clusters were chosen for k-means clustering. An Activity Index (AV) was created based on the clustering, ranging from 0 (minimal activity) to 6 (maximal activity). AV data was visualised using the plot and ring commands of the dphenome module (Fig. S2).

In vitro growth experiments

Briefly, for individual growth curves, 10 ml of either LB-Lennox or defined minimal medium was inoculated with 20 µl of a culture grown overnight in LB-Lennox broth. Cultures were grown at 37 °C with shaking at 200 RPM and samples were removed at regular intervals to measure bioluminescence, using a VICTOR X Light Plate reader (Perkin Elmer), and viable counts, by plating onto LB-Lennox Agar (Fort Richard Laboratories Ltd., Auckland, New Zealand). Overnight cultures were plated to determine the initial inocula. Experiments were performed on seven separate occasions and results used to calculate area under curve (AUC) values for each strain. For the competition experiments, 10 µl of a culture grown overnight in LB-Lennox broth was used to inoculate 1 ml of defined minimal medium, with the mixed culture tubes receiving 5 µl of each strain. Inoculated tubes were incubated overnight at 37 °C with shaking at 200 RPM, followed by serial dilution in sterile phosphate buffered saline (PBS) for plating onto LB Agar containing either nalidixic acid or kanamycin. The ratio of colonies that grew on media containing each antibiotic was used to determine the proportion of each strain remaining. Experiments were performed on eight separate occasions and the results used to calculate AUC values and competitive indices (CI). CI's were calculated as follows: CI = [strain of interest output/competing strain output]/[strain of interest input/competing strain input] (*Freter, O'Brien & Macsai*, *1981*; *Taylor et al.*, *1987*).

Infection of *Galleria mellonella*

5th instar *Galleria mellonella* larvae (waxworms) were obtained from a commercial supplier (Biosuppliers.com, Auckland, New Zealand). Bacteria were grown overnight in LB-Lennox broth and used to infect waxworms which were pale in colour and weighed approximately 100–200 mg. Waxworms were injected into one of the last set of prolegs with 20 µl of approximately 10^8 colony forming units (CFU) of bacteria using a 1ml fine needle insulin syringe. Waxworms were injected with either ICC169, ICC180 or a 1:1 mix and incubated at 37 °C. Throughout the course of a 24 h infection, individual waxworms were inspected for phenotypic changes and scored using a standardised method for assessing waxworm health (the Caterpillar Health Index [CHI]) which we have developed. Briefly, waxworms were monitored for movement, cocoon formation, melanisation, and survival. Together, these data form a numerical scale, with lower CHI scores corresponding with more serious infections and higher scores with healthier waxworms. Scores were used to calculate AUC values. Bioluminescence (given as relative light units [RLU]) was measured at regular intervals from waxworms infected with ICC180 (Fig. S3). Waxworms were placed into individual wells of a dark OptiPlate-96 well microtitre plate (Perkin Elmer) and bioluminescence measured for 1 s to provide relative light units (RLU)/second using the VICTOR X Light Plate reader. Waxworms infected with ICC169 were used as a control.

Following death, or at 24 h, waxworms were homogenised in PBS and plated onto LB-Lennox Agar containing the appropriate antibiotics. Independent experiments were performed three times using 10 waxworms per group.

Infection of Mice

Female 6–7 week old C57BL/6Elite mice were provided by the Vernon Jansen Unit (University of Auckland) from specific-pathogen free (SPF) stocks. All animals were housed in individually HEPA-filtered cages with sterile bedding and free access to sterilised food water. Experiments were performed in accordance with the New Zealand Animal Welfare Act (1999) and institutional guidelines provided by the University of Auckland Animal Ethics Committee, which reviewed and approved these experiments under applications R1003 and R1496. Bacteria grown overnight in LB-Lennox broth were spun at 4500 RPM for 5 min, and resuspended in a tenth of the volume of sterile PBS, producing a 10x concentrated inoculum. Animals were orally inoculated using a gavage needles with 200 μl of either ICC169, ICC180, or a 1:1 mix (containing approximately 10^8 CFU of bacteria) and biophotonic imaging used to determine correct delivery of bacteria to the stomach. The number of viable bacteria used as an inoculum was determined by retrospective plating onto LB-Lennox Agar containing either nalidixic acid or kanamycin. Stool samples were recovered aseptically at various time points after inoculation, and the number of viable bacteria per gram of stool was determined after homogenisation at 0.1 g ml^{-1} in PBS and plating onto LB-Lennox Agar containing the appropriate antibiotics. The number and ratio of colonies growing on each antibiotic was used to calculate AUC values and CI's as described above. Independent experiments were performed twice using 6 animals per group.

In vivo bioluminescence imaging

Biophotonic imaging was used to noninvasively measure the bioluminescent signal emitted by *C. rodentium* ICC180 from anaesthetised mice to provide information regarding the localisation of the bacterium. Prior to being imaged, the abdominal area of each mouse was shaved, using a Vidal Sasoon handheld facial hair trimmer, to minimise any potential signal impedance by melanin within pigmented skin and fur. Mice were anaesthetised with gaseous isoflurane and bioluminescence (given as photons s^{-1} cm^{-2} steradian $[sr]^{-1}$) was measured using the IVIS® Kinetic camera system (Perkin Elmer). A photograph (reference image) was taken under low illumination before quantification of photons emitted from ICC180 at a binning of four over 1 min using the Living Image software (Perkin Elmer). The sample shelf was set to position D (field of view, 12.5 cm). For anatomic localisation, a pseudocolor image representing light intensity (blue, least intense to red, most intense) was generated using the Living Image software and superimposed over the gray-scale reference image. Bioluminescence in specific regions of individual mice also was quantified using the region of interest tool in the Living Image software program (given as photons s^{-1}) and used to calculate AUC values for each individual animal.

Statistical analyses

Data was analysed using GraphPad Prism 6. Data was tested for normality using the D'Agostino-Pearson test; data which failed normality was analysed using a non-parametric

Table 1 SNPs and indels that differ between the bioluminescent *C. rodentium* derivative ICC180 and its parent strain ICC169. Sequencing revealed three points of difference between ICC180 and ICC169. Two SNPs are present, each cytosine substitutions, and one guanine insertion inducing a frameshift mutation. Sequencing data was analysed using BreSeq (*Deatherage & Barrick*, *2014*).

Position	Base change	Amino acid change	Gene	Function
2,936,285	T→C	D471G (GAC→GGC)	*cts1V*	T6SS protein Cts1V
3,999,002	T→C	E89G (GAG→GGG)	*pflD*	Formate acetyltransferase 2
3,326,092	CAG→CAGG	Frameshift	*ROD_31611*	Major Facilitator Superfamily transporter

test, while data which passed normality was analysed using a parametric test. One-tailed tests were used to test the hypothesis that constitutively expressing light gives ICC180 a differential fitness cost compared to the non-bioluminescent parent strain ICC169. When comparing multiple experimental groups, Dunn's post hoc multiple comparison test was applied.

RESULTS

Bioluminescent *Citrobacter rodentium* strain ICC180 has three altered chromosomal genes and a large deletion in plasmid pCROD1 in addition to insertion of the *lux* operon and kanamycin resistance gene

We determined the whole genome draft sequences of *C. rodentium* ICC169 and ICC180 using Illumina sequence data. Compared with sequenced type strain ICC168 (Genbank accession number FN543502.1), both strains have a substitution of a guanine (G) to an adenine (A) residue at 2,475,894 bp, resulting in an amino acid change from serine (Ser) to phenylalanine (Phe) within *gyrA*, the DNA gyrase subunit, and conferring resistance to nalidixic acid. The sequencing data indicate that the *lux* operon and kanamycin resistance gene (a 7,759 bp fragment) has inserted at 5,212,273 bp, disrupting the coding region of a putative site-specific DNA recombinase (Fig. 1). In addition to the presence of the *lux* operon and kanamycin resistance gene, we found that the genome of ICC180 differs from ICC169 by two single nucleotide polymorphisms (SNPs), a single base pair insertion (of a G residue at 3,326,092 bp which results in a frameshift mutation within *ROD*_31611, a putative membrane transporter) and a 90 bp deletion in *deoR* (deoxyribose operon repressor) (Table 1). All four plasmids previously described for *C. rodentium* were present in ICC180, however the largest of these plasmids, pCROD1, shows evidence of extensive deletion events and is missing 41 out of 60 genes (Table S2).

Constitutive light expression does not greatly impact the metabolism of *C. rodentium* ICC180

C. rodentium ICC169 and its bioluminescent derivative ICC180 were grown on two separate occasions using PM plates 1–20. We analysed the data using the DuctApe software suite which calculates an activity index (AV) for each strain in response to each well (Fig. S2). Next, the growth curve data were transformed into Signal Values (SVs) as previously described (*Reuter*

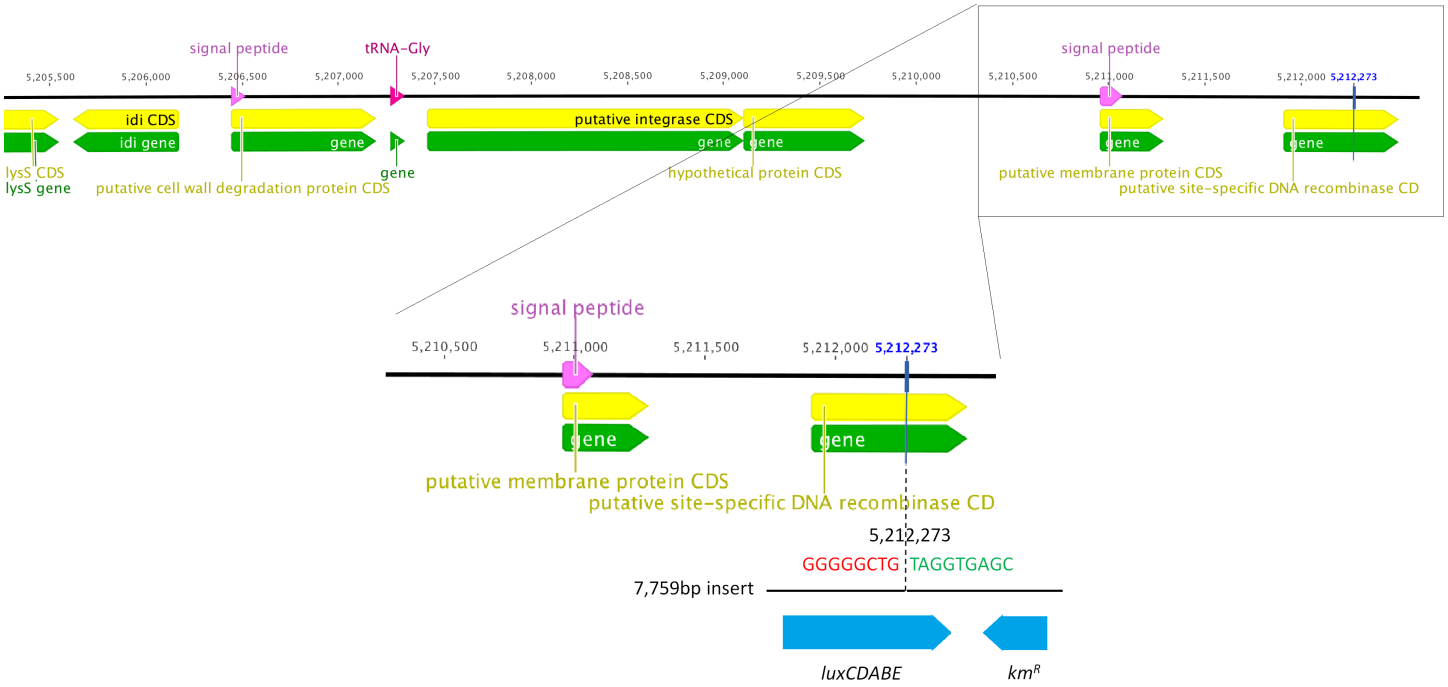

Figure 1 Whole genome sequencing shows that the *lux* operon and kanamcyin resistance gene have inserted at position 5,212,273 in the chromosome of *C. rodentium* ICC180, disrupting a putative site-specific DNA recombinase.

et al., *2014*), summarising the growth of each strain over time for each well. Wells which were considered to be actively respiring were analysed using the moderated *t*-test implemented in the limma R/Bioconductor package (*Smyth*, *2004*). Those wells with a Benjamini–Hochberg corrected *P*-value of less than 0.05 are shown in Table 2 (with corresponding growth curves in Fig. 3). Our results indicate that the growth of the two strains significantly differed ($p = < 0.05$) in 26/1,920 wells. Of these >80% are from the PM11-20 plates, which belong to the chemical category, suggesting that the expression of bioluminescence is near-neutral in almost every non-toxic environment. The bioluminescent strain ICC180 is able to use D-glucosamine, cytidine and Ala-His as nitrogen sources, and inositol hexaphosphate as a phosphate source, and grew significantly better than ICC169 in the presence of 11 chemicals: the antibiotics kanamycin, paromomycin, geneticin, spiramycin, rolitetracycline, doxycycline, cefoxitin; the quaternary ammonium salt dequalinium chloride; coumarin; iodonitrotetrazolium violet; and the acetaldehyde dehydrogenase inhibitor disulphiram (Table 2). That the expression of a kanamycin resistance gene also improves growth of ICC180 in the presence of related aminoglycosides is reassuring. In contrast, the wildtype strain ICC169 was able to use the nitrogen peptide Lys-Asp and grew significantly better in the presence of 8 chemicals: the metal chelators, EDTA and EGTA, sodium nitrate, the antibiotics rifampicin and phenethicillin, the fungicide oxycarboxin, the cyclic polypeptide colistin, the nucleoside analogue cytosine-1-b-D-arabinofuranoside and (Table 2). The fact that significant differences in growth rate were observed for so few conditions, provided robust and comprehensive evidence that light production is near-neutral in *C. rodentium* ICC180.

Table 2 Phenotypic microarray (PM) wells in which the growth of bioluminescent *C. rodentium* derivative ICC180 significantly differs from its non-bioluminescent parent strain ICC169.

PM class	Substrate	Adjusted *P* value	Improved growth by ICC169	Improved growth by ICC180	Comment
Nitrogen	D-glucosamine	0.0159		√	
	Cytidine	0.0280		√	
	Ala-His	0.0316		√	
Phosphate	Inositol hexaphosphate	0.0280		√	
Nitrogen peptides	Lys-Asp	0.0306	√		
Chemicals	Kanamycin	0.0076		√	Conferred by KanR gene
	Paromomycin	0.0048		√	Aminoglycoside—the kanamycin cassette will be mediating resistance
	Geneticin	0.0048		√	Aminoglycoside—the kanamycin cassette will be mediating resistance
	Dequalinium chloride	0.0116		√	Quaternary ammonium salt
	Spiramycin	0.0088		√	Macrolide—acts at ribosomal 50S, c.f. aminoglycosides at 30S
	Rolitetracycline	0.0316		√	Tetracycline; prevents tRNA binding at 30S A-site
	Doxycycline	0.0210		√	Tetracycline; prevents tRNA binding at 30S A-site
	Coumarin	0.0333		√	Fragrant organic compound found in many plants
	Iodonitro tetrazolium violet (INT)	0.0087		√	Electron acceptor, reduced by succinate dehydrogenase (and by superoxide radicals)
	EDTA	0.0048	√		Metal chelator
	EGTA	0.0210	√		Metal chelator
	Rifampicin	0.0048	√		RNA polymerase inhibitor
	Colistin	0.0048	√		Cyclic polypeptide; disrupts outer membrane
	Oxycarboxin	0.0121	√		Fungicide
	Phenethicillin	0.0048	√		Beta-lactam

(*continued on next page*)

Table 2 (*continued*)

PM class	Substrate	Adjusted *P* value	Improved growth by ICC169	Improved growth by ICC180	Comment
	Cytosine-1-b-D-arabinofuranoside	0.0123	√		Nucleoside analogue (anti-cancer/-viral)
	Sodium Nitrate	0.0306	√		
	Cefoxitin	0.0316		√	Beta-lactam
	Disulphiram	0.0349		√	Inhibits acetaldehyde dehydrogenase

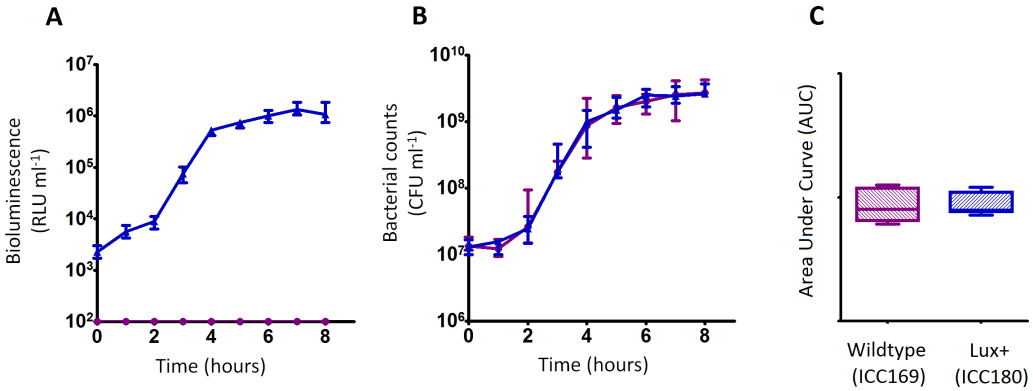

Figure 2 ***C. rodentium*** **ICC180 is not impaired during growth in a rich laboratory medium when compared to its non-bioluminescent parent strain ICC169.** Wildtype *C. rodentium* ICC169 (shown as purple circles) and its bioluminescent derivative ICC180 (shown as blue triangles) were grown in LB-Lennox broth and monitored for changes in bioluminescence (given as relative light units [RLU] ml^{-1}) (A) and bacterial counts (given as colony forming units [CFU] ml^{-1}) (B). Bacterial count data was used to calculate area under curve (AUC) values for each strain (C). Data (medians with ranges where appropriate) is presented from experiments performed on eight separate occasions.

The growth of ICC180 is not impaired in a rich laboratory medium, when compared to its non-bioluminescent parent strain, but does exhibit an increased lag phase when grown in a restricted medium

We grew ICC180 and ICC169 in rich (LB-Lennox) and restricted (minimal A salts with 1% glucose supplementation) laboratory media. For ICC180, we found that bioluminescence strongly correlated with the bacterial counts recovered throughout the growth period in both LB-Lennox (Spearman's $r = 0.9293$ 95% CI [0.8828–0.9578], $p = < 0.0001$) and the restricted medium (Spearman's $r = 0.9440$ 95% CI [0.9001–0.9689], $p = < 0.0001$) (Figs. 2A, 2B, 3A &3B). We also found that the growth of each strain was comparable in LB-Lennox medium, with no significant difference between the bacterial counts recovered over 8 h (Fig. 2B), as demonstrated by the calculated AUC values (Fig. 2C).

We also found no significant difference between the bacterial counts recovered from ICC180 and ICC169 growing in the restricted medium for 14 h (mean CFU 5.67×10^8 [SD 2.31×10^8] and 8.84×10^8 [SD 2.93×10^8], respectively). However, we did find a significant difference between the AUC values calculated from the bacterial counts recovered over the course of 14 h ($p = 0.0078$, one-tailed Wilcoxon matched-pairs signed rank test)

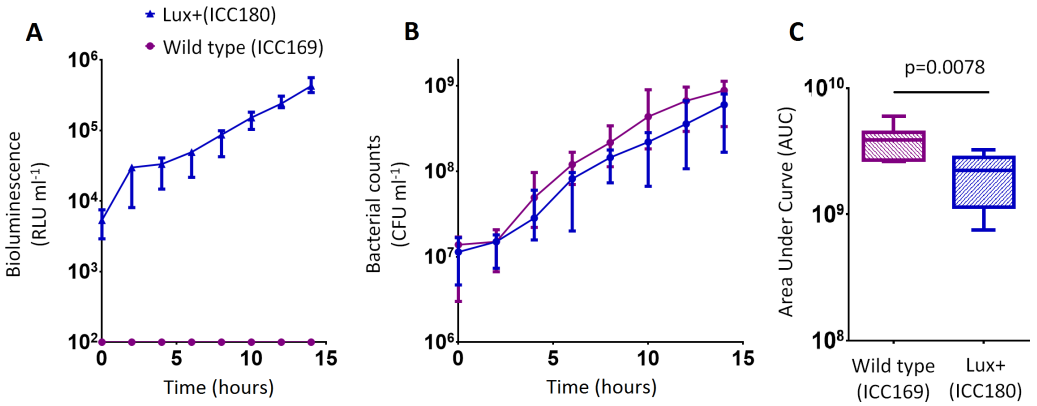

Figure 3 ***C. rodentium*** **ICC180 is mildly impaired during growth in a defined minimal laboratory medium when compared to its non-bioluminescent parent strain ICC169.** Wildtype *C. rodentium* ICC169 (shown as purple circles) and its bioluminescent derivative ICC180 (shown as blue triangles) were grown in minimal A salts supplemented with 1% glucose and monitored for changes in bioluminescence (given as relative light units [RLU] ml^{-1}) (A) and bacterial counts (given as colony forming units [CFU] ml^{-1}) (B). Bacterial count data was used to calculate area under curve (AUC) values for each strain, which were found to be significantly different ($p = 0.0078$; Wilcoxon Matched pairs-signed rank test) (C). Data (medians with ranges where appropriate) is presented from experiments performed on eight separate occasions.

(Fig. 3C). We calculated the slopes of the growth curves and found that there was no difference in the rates of growth of the two strains during exponential phase. Instead, we found a significant difference between the slopes calculated during the first 4 h of growth (1/slope values: ICC169 $= 1.48\times10^{-7}$ [SD 9.98×10^{-8}], ICC180 $= 2.47\times10^{-7}$ [SD 1.10×10^{-7}]; $p = 0.0041$, one-tailed Paired t test), suggesting ICC180 spends longer in lag phase than ICC169 when grown in the restricted medium used.

ICC180 is not impaired in the *Galleria mellonella* infection model

We infected larvae of the Greater Wax Moth *G. mellonella* (waxworms) with ICC169 and ICC180 in single and 1:1 mixed infections. We monitored the waxworms over a 24–48 h period for survival and disease symptoms. The Caterpillar Health Index (CHI) is a numerical scoring system which measures degree of melanisation, silk production, motility, and mortality. We found that the majority of infected waxworms succumb to *C. rodentium* infection (Fig. 4A), which is reflected by the concurrent decrease in CHI score (Fig. 4B). This is in contrast to waxworms injected with PBS, who all survived and consistently scored 9–10 on the CHI scale throughout the experiments. We also found that the survival and symptoms of waxworms infected with each strain were comparable, with no significant difference between the survival curves (Fig. 4A), and calculated AUC values for the CHI scores (Fig. 4C). However, when we directly compared ICC169 and ICC180 in mixed infections of approximately 1:1, we found a significant difference in the relative abundance of the bacteria recovered from waxworms at either time of death or 24 h, whichever occurred first ($p = 0.001$, one-tailed Wilcoxon matched-pairs signed rank test). Despite a slightly lower infectious dose, higher numbers of ICC180 were consistently recovered from infected waxworms (Fig. 4D).

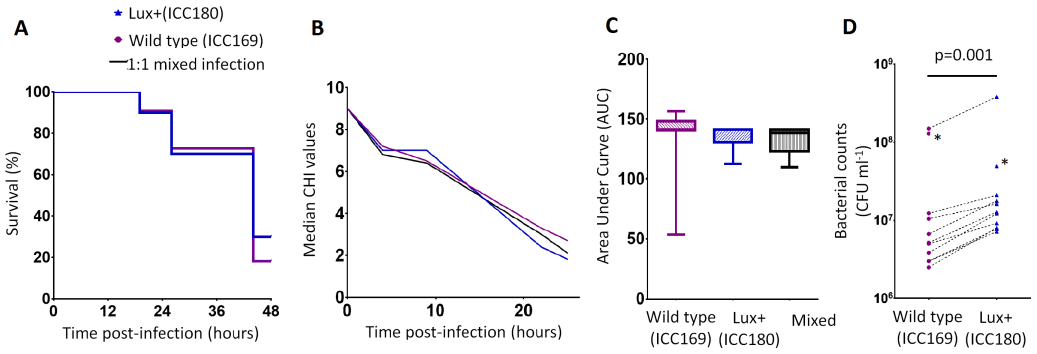

Figure 4 Bioluminescent *C. rodentium* ICC180 is not impaired in the *Galleria mellonella* infection model. Groups of larvae ($n = 10$) of the Greater Wax Moth *Galleria mellonella* were infected with ICC169 and ICC180 in single and 1:1 mixed infections and monitored for survival (%) (A) and for disease symptoms using the Caterpillar Health Index (CHI), a numerical scoring system which measures degree of melanisation, silk production, motility, and mortality (given as median CHI values) (B). Survival curves (A) and calculated area under curve (AUC) data of CHI scores reveals no difference between waxworm response to infection from either strain (C). Waxworms infected with a 1:1 mix of ICC169 and ICC180 were homogenised at 24-hours, or at time of death if earlier. Actual infecting doses for each strain were determined by retrospective plating, and are indicated by *. The bacterial burden of ICC180 and ICC169 in individual caterpillars (indicated by the dotted line), was calculated after plating onto differential media and found to be significantly different ($p = 0.001$; one-tailed Wilcoxon matched pairs-signed rank test) (D). Data (medians with ranges where appropriate) is presented from experiments performed on three separate occasions, except (A) and (D), where the results of a representative experiment are shown.

ICC180 is impaired in mixed but not in single infections in mice when compared to its non-bioluminescent parent strain

We orally gavaged groups of female 6–8 week old C57Bl/6 mice ($n = 6$) with $\sim 5 \times 10^9$ CFU of ICC169 and ICC180, either individually or with a 1:1 ratio of each strain. We followed the infection dynamics by obtaining bacterial counts from stool samples (Fig. 5) and by monitoring bioluminescence from ICC180 using biophotonic imaging (Fig. 6). We found that the growth of each strain was comparable during single infections, with no significant difference between the bacterial counts recovered throughout the infection (Fig. 5A), as demonstrated by the calculated AUC values (Fig. 5B).

In contrast, we found a significant difference between the AUC values calculated from the bacterial counts recovered from ICC180 and ICC169 during mixed infections ($p = 0.001$, one-tailed Wilcoxon matched-pairs signed rank test) (Fig. 5D). Our data demonstrates that when in direct competition with ICC169, ICC180 is shed at consistently lower numbers from infected animals (Fig. 5C). At the peak of infection (days 6–8), this equates to over a 10-fold difference, with mice shedding a median of 1.195×10^8 CFU (SD 4.544×10^7) for ICC169 compared to 9.98×10^6 CFU (SD 1.544×10^7) for ICC180. This disadvantage is reflected in the Competitive Indices we calculated from bacterial counts recovered at each time point, which for ICC180 decreased steadily throughout the course of the infection (Fig. 5E). Despite this disadvantage, ICC180 is never completely outcompeted and remains detectable in the stools of infected animals until the clearance of infection (Fig. 5C), and by biophotonic imaging until day 10–13 post-infection (Fig. 6A).

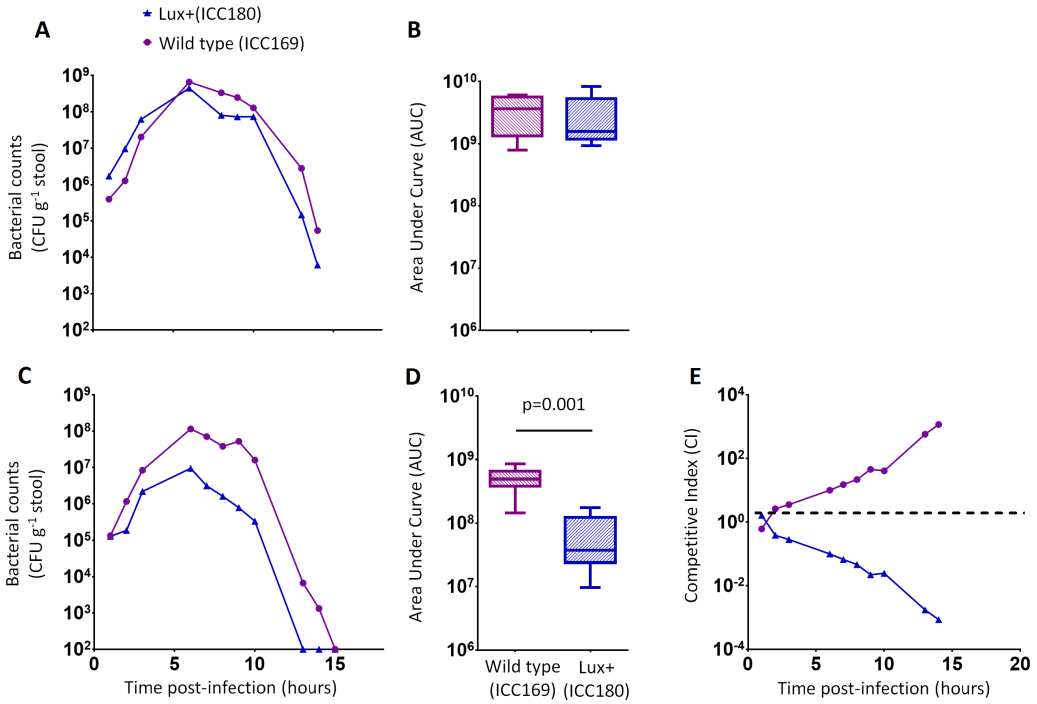

Figure 5 ***C. rodentium*** **ICC180 is impaired during mixed, but not in single, infections in mice when compared to its non-bioluminescent parent strain ICC169.** Groups of female 6–8 week old C57Bl/6 mice ($n = 6$) were orally-gavaged with $\sim 5 \times 10^9$ CFU of wildtype *C. rodentium* ICC169 (shown as purple circles) and its bioluminescent derivative ICC180 (shown as blue triangles) in single infections (A, B) or 1:1 mixed infections (C, D) and monitored for changes in bacterial counts (given as colony forming units [CFU] g^{-1} stool) (A, B). Bacterial count data was used to calculate area under curve (AUC) values for each strain in single (B) and mixed (D) infections, and were found to be significantly different only for the mixed infections ($p = 0.001$; one-tailed Wilcoxon Matched pairs-signed rank test). This is reflected in the competitive indices (CI) calculated from the bacterial counts recovered during mixed infections, with ICC180 showing a growing competitive disadvantage from day 2 post-infection (E). Data (medians with ranges where appropriate) is presented from experiments performed on two separate occasions.

DISCUSSION

Bioluminescently-labelled bacteria have gained popularity as a powerful tool for investigating microbial pathogenicity *in vivo*, and for preclinical drug and vaccine development (*Steinhuber et al.*, *2008*; *Massey et al.*, *2011*; *Sun et al.*, *2012*; *Kassem et al.*, *2016*). Individual infected and/or treated animals can be followed over time, in contrast to the large numbers of animals that are euthanised at specific time points of interest for quantifying bacterial loads using labour-intensive plate count methods. Most widely used is the *lux* operon of the terrestrial bacterium *P. luminescens*, which encodes for the luciferase enzyme which catalyses the bioluminescence reaction, and for a multi-enzyme complex responsible for regenerating the required substrate. As $FMNH_2$ is also required for light production, it is generally hypothesised that light production is likely to impose a metabolic burden on tagged bacteria.

The impact of expression of the *lux* operon has been reported for a number of microbial species. Sanz and colleagues (*2008*) created strains of *Bacillus anthracis* that emit light

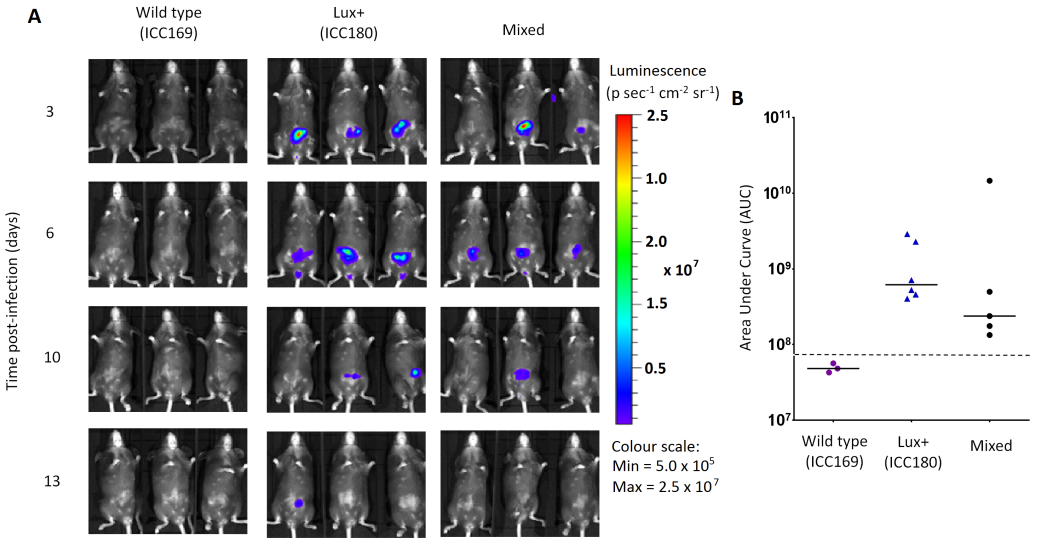

Figure 6 Despite having a fitness disadvantage in mixed infections of mice, ICC180 is still visible by biophotonic imaging. Groups of female 6–8 week old C57Bl/6 mice ($n = 6$) were orally-gavaged with $\sim 5\times10^9$ CFU of wildtype *C. rodentium* ICC169 and its bioluminescent derivative ICC180 in single infections or 1:1 mixed infections. Mice were anaesthetised with gaseous isoflurane and bioluminescence (given as photons s^{-1} cm^{-2} sr^{-1}) from ICC180 measured using the IVIS® Kinetic camera system (Perkin Elmer). The images show changes in peak bioluminescence over time with variations in colour representing light intensity at a given location and superimposed over a grey-scale reference image (A). Red represents the most intense light emission, whereas blue corresponds to the weakest signal. Bioluminescence from the abdominal region of individual mice was quantified (as photons s^{-1}) using the region of interest tool in the Living Image software program and used to calculate area under curve (AUC) values for each individual animal over the course of the infection (B). Dotted line represents background. Experiments were performed on two separate occasions. Three representative animals are shown; no light was detected from animals infected with ICC169 alone, while lower levels of light were detected from animals infected with a mix of ICC169 and ICC180.

during germination, by introducing plasmids with *lux* operon expression driven by the *sspB* promoter. The authors noted that the bioluminescent strains were less efficient at germinating, resulting in an increase in the dose required to cause a lethal infection in mice inoculated by either the subcutaneous or intranasal route. Despite the reduced virulence, bioluminescent *B. anthracis* was still capable of successfully mounting an infection, and the use of biophotonic imaging revealed new infection niches which would have been difficult to accurately measure using traditional plating methods. Similarly, a clinical M75 isolate of *Streptococcus pyogenes* with the *lux* operon chromosomally inserted at the *spy0535* gene was found to have significantly attenuated maximal growth *in vitro*, as well as reduced survival in an intranasal mouse model (*Alam et al.*, *2013*). The bioluminescent *Listeria monocytogenes* Xen32 strain was shown to cause reduced mortality after oral inoculation of BALB/cJ mice, however subsequent investigation revealed that the chromosomally-located *lux* operon had inserted into the *flaA* gene, disrupting the ability of Xen32 to produce flagella. This suggests that the virulence attenuation observed is likely due to the location of the *lux* operon rather than the metabolic cost of light production (*Bergmann et al.*, *2013*).

In this study, we compared a bioluminescent-derivative of the mouse enteropathogen *C. rodentium*, strain ICC180, with its non-bioluminescent parent strain ICC169, using

the BIOLOG Phenotypic Microarray (PM) system, which tests microbial growth under approximately 2,000 different metabolic conditions. Rather surprisingly, our results demonstrated that the expression of bioluminescence in ICC180 is near-neutral in almost every non-toxic environment tested, suggesting that light production is not metabolically costly to *C. rodentium*. This supports the "free lunch hypothesis" proposed by Falls and colleagues (*2014*), namely that cells have an excess of metabolic power available to them. Interestingly, ICC180 grew significantly better than its non-bioluminescent parent strain in the presence of a number of different chemicals, including several antibiotics, supporting previous findings that bacteria have many pleiotropic ways to resist toxins (*Soo, Hanson-Manful & Patrick*, *2011*). In the case of the artificial electron acceptor iodonitrotetrazolium violet, we hypothesise that light production may be altering the redox balance of the cell, thus making the dye less toxic.

We also compared the ability of ICC180 and ICC169 to directly compete with one another during infection of their natural host, laboratory mice, as well as larvae of the Greater Wax Moth *G. mellonella* (waxworms). Wax worms are becoming an increasingly popular surrogate host for infectious diseases studies due to legislative requirements in many countries to replace the use of animals in scientific research. Wax worms have a well-developed innate immune system involving a cellular immune response in the form of haemocytes, and a humoral immune response in the form of antimicrobial peptides in the hemolymph (*Vogel et al.*, *2011*). Detection of bacterial cell wall components leads to activation of the prophenoloxidase cascade, which is similar to the complement system in mammals (*Park et al.*, *2005*), and subsequent endocytosis of bacteria by haemocytes. The haemocytes function in a similar way to mammalian neutrophils, and kill bacteria via NADPH oxidase and production of reactive oxygen species (*Bergin et al.*, *2005*). Again, we observed no fitness costs to constitutive light production by ICC180. Interestingly, we recovered significantly more ICC180 from wax worms infected with both ICC180 and ICC169. Similar to the response to iodonitrotetrazolium violet, an altered redox balance caused by light production could make reactive oxygen species generated by the wax worm immune response, less toxic.

In contrast, our data shows that the non-bioluminescent parent strain ICC169 has a clear competitive advantage over ICC180 during infection of adult C57Bl/6 mice, with the bioluminescent strain shed from infected animals at consistently lower numbers. Surprisingly though, this competitive advantage is not sufficient for the parent strain to entirely outcompete and displace its bioluminescent derivative, which remains present in the gastrointestinal tract until clearance of both strains by the immune system. This suggests that there are sufficient niches within the gastrointestinal tract for the two strains to coexist.

It is important to note that in addition to light production, ICC180 differs from its non-bioluminescent parent strain ICC169 by lacking a putative site-specific DNA recombinase, disrupted by insertion of the *lux* operon. *C. rodentium* ICC180 was constructed by random transposon mutagenesis of ICC169 with a mini-Tn5 vector containing an unpromoted *lux* operon and kanamycin-resistance gene. Previous characterisation of the site of insertion of the *lux* operon suggested that the transposon had inserted within a homologue of the *xylE* gene. However, whole genome sequencing has revealed that this was incorrect and

the *lux* operon has inserted at 5,212,273 bp, disrupting the coding region of the putative site-specific DNA recombinase. Whole genome sequencing also revealed that ICC180 differs from ICC169 by 2 non-synonymous SNPs, a single base pair insertion and a 90 bp deletion. It is unclear if these changes occurred during the process of transposon mutagenesis, and are merely 'hitch-hikers,' or after laboratory passage. The single base pair insertion revealed by sequencing is of a G residue at 3,326,092 bp which results in a frameshift mutation within a putative membrane transporter, while the 90 bp deletion is within the deoxyribose operon repressor gene *deoR*. The DeoR protein represses the *deoCABD* operon, which is involved in the catabolism of deoxyribonucleotides. One SNP is the substitution of an aspartic acid (D) for a glycine (G) at residue 471 of Cts1V, a Type 6 secretion system protein involved in ATP binding. The other SNP is the substitution of a glutamic acid (E) for a glycine (G) at residue 89 of the formate acetyletransferase 2 gene *pflD*, which is involved in carbon utilisation under anaerobic conditions. Modelling suggests that once mutated, residue 89 will be unable to make several key contacts, suggesting the function of PflD will be affected. As we have not introduced these genetic differences into the non-bioluminescent parent strain, we cannot be certain whether the fitness costs we observed are a result of any single or combination of these differences, or expression of the *lux* operon. In addition, at 54 kb the largest *C. rodentium* plasmid pCROD1 is dramatically altered in ICC180, missing 41 out of 60 of genes. This is in contrast to previous results which indicated that pCROD1 is entirely absent in ICC180 (*Petty et al.*, *2011*). We do not anticipate that the loss of a large part of this plasmid will have any significant impact however, as it has been shown that pCROD1 is frequently lost in *C. rodentium*, and that strains lacking pCROD1 do not show any attenuation of virulence in a C57BL/6 mouse model (*Petty et al.*, *2011*).

In conclusion, the bioluminescent *C. rodentium* strain ICC180 has a clear disadvantage when directly competed with its parent stain in mice. However, the fact that it reaches similar numbers, and causes similar pathology (*Wiles et al.*, *2005*; *Wiles et al.*, *2006*), during single infections is reassuring. Our phenotypic microarray data suggests that constitutive light expression is surprisingly neutral in *C. rodentium* and supports the view that bioluminescent versions of microbes can be used as a substitute for their non-bioluminescent parents, at least in theory. In reality, the actual fitness costs will likely depend on the host bacterial species, whether the *lux* operon is located on a multi-copy plasmid or integrated into the chromosome (and if chromosomal, the site of insertion of the operon), and the levels of expression of the *lux* genes.

ADDITIONAL INFORMATION AND DECLARATIONS

Funding

This work was supported by seed funding from the Maurice Wilkins Centre for Molecular Biodiscovery, and by a Sir Charles Hercus Fellowship to SW (09/099) from the Health Research Council of New Zealand. LB is supported by a Research Fellowship from the Alexander von Humboldt Stiftung/Foundation. The funders had no role in study design, data collection and analysis, decision to publish, or preparation of the manuscript.

Grant Disclosures

The following grant information was disclosed by the authors:
Maurice Wilkins Centre for Molecular Biodiscovery.
Health Research Council of New Zealand: SW (09/099).
Alexander von Humboldt Stiftung/Foundation.

Competing Interests

Siouxsie Wiles is an Academic Editor for PeerJ.

Author Contributions

- Hannah M. Read conceived and designed the experiments, performed the experiments, analyzed the data, wrote the paper, prepared figures and/or tables, reviewed drafts of the paper.
- Grant Mills and Sarah Johnson performed the experiments, reviewed drafts of the paper.
- Peter Tsai analyzed the data, prepared figures and/or tables, reviewed drafts of the paper.
- James Dalton performed the experiments, analyzed the data, reviewed drafts of the paper.
- Lars Barquist analyzed the data, contributed reagents/materials/analysis tools, reviewed drafts of the paper.
- Cristin G. Print contributed reagents/materials/analysis tools, reviewed drafts of the paper.
- Wayne M. Patrick analyzed the data, reviewed drafts of the paper.
- Siouxsie Wiles conceived and designed the experiments, performed the experiments, analyzed the data, contributed reagents/materials/analysis tools, wrote the paper, prepared figures and/or tables, reviewed drafts of the paper.

Animal Ethics

The following information was supplied relating to ethical approvals (i.e., approving body and any reference numbers):

Experiments were performed in accordance with the New Zealand Animal Welfare Act (1999) and institutional guidelines provided by the University of Auckland Animal Ethics Committee, which reviewed and approved these experiments under applications R1003 and R1496.

DNA Deposition

The following information was supplied regarding the deposition of DNA sequences:

GenBank: SRP076686.

Data Availability

The following information was supplied regarding data availability:

Figshare: https://dx.doi.org/10.17608/k6.auckland.3407935.v1.

Supplemental Information

Supplemental information for this article can be found online at http://dx.doi.org/10.7717/peerj.2130#supplemental-information.

REFERENCES

Alam FM, Bateman C, Turner CE, Wiles S, Sriskandan S. 2013. Non-invasive monitoring of *Streptococcus pyogenes* vaccine efficacy using biophotonic imaging. *PLoS ONE* **8**:e82123 DOI 10.1371/journal.pone.0082123.

Andreu N, Fletcher T, Krishnan N, Wiles S, Robertson BD. 2012. Rapid measurement of antituberculosis drug activity *in vitro* and in macrophages using bioluminescence. *Journal of Antimicrobial Chemotherapy* **67**:404–414 DOI 10.1093/jac/dkr472.

Andreu N, Zelmer A, Sampson SL, Ikeh M, Bancroft GJ, Schaible UE, Wiles S, Robertson BD. 2013. Rapid *in vivo* assessment of drug efficacy against *Mycobacterium tuberculosis* using an improved firefly luciferase. *Journal of Antimicrobial Chemotherapy* **68**:2118–2127 DOI 10.1093/jac/dkt155.

Andreu N, Zelmer A, Wiles S. 2011. Noninvasive biophotonic imaging for studies of infectious disease. *FEMS Microbiology Reviews* **35**:360–394 DOI 10.1111/j.1574-6976.2010.00252.x.

Bergin D, Reeves E, Renwick J, Wientjes F, Kavanagh K. 2005. Superoxide production in *Galleria mellonella* hemocytes: identification of proteins homologous to the NADPH oxidase complex of human neutrophils. *Infection and Immunity* **73**:4161–4170 DOI 10.1128/IAI.73.7.4161-4170.2005.

Bergmann S, Rohde M, Schughart K, Lengeling A. 2013. The bioluminescent *Listeria monocytogenes* strain Xen32 is defective in flagella expression and highly attenuated in orally infected BALB/cJ mice. *Gut Pathogens* **5**:19 DOI 10.1186/1757-4749-5-19.

Bochner BR, Gadzinski P, Panomitros E. 2001. Phenotype microarrays for high-throughput phenotypic testing and assay of gene function. *Genome Research* **11**:1246–1255 DOI 10.1101/gr.186501.

Collins JW, Keeney KM, Crepin VF, Rathinam VA, Fitzgerald KA, Finlay BB, Frankel G. 2014. *Citrobacter rodentium*: infection, inflammation and the microbiota. *Nature Reviews Microbiology* **12**:612–623 DOI 10.1038/nrmicro3315.

Cox MP, Peterson DA, Biggs PJ. 2010. SolexaQA: at-a-glance quality assessment of illumina second-generation sequencing data. *BMC Bioinformatics* **11**:485 DOI 10.1186/1471-2105-11-485.

Davis BD. 1949. The isolation of biochemically deficient mutants of bacteria by means of penicillin. *Proceedings of the National Academy of Sciences of the United States of America* **35**:1–10 DOI 10.1073/pnas.35.1.1.

De Wet JR, Wood KV, Helinski DR, Deluca M. 1985. Cloning of firefly luciferase cDNA and the expression of active luciferase in *Escherichia coli*. *Proceedings of the National Academy of Sciences of the United States of America* **82**:7870–7873 DOI 10.1073/pnas.82.23.7870.

Deatherage DE, Barrick JE. 2014. Identification of mutations in laboratory-evolved microbes from next-generation sequencing data using breseq. *Methods in Molecular Biology* **1151**:165–188 DOI 10.1007/978-1-4939-0554-6_12.

Engebrecht J, Nealson K, Silverman M. 1983. Bacterial bioluminescence: isolation and genetic analysis of functions from *Vibrio fischeri*. *Cell* **32**:773–781.

Falls K, Williams A, Bryksin A, Matsumura I. 2014. *Escherichia coli* deletion mutants illuminate trade-offs between growth rate and flux through a foreign anabolic pathway. *PLoS ONE* **9**:e88159 DOI 10.1371/journal.pone.0088159.

Freter R, O'Brien PC, Macsai MS. 1981. Role of chemotaxis in the association of motile bacteria with intestinal mucosa: *in vivo* studies. *Infection and Immunity* **34**:234–240.

Galardini M, Mengoni A, Biondi EG, Semeraro R, Florio A, Bazzicalupo M, Benedetti A, Mocali S. 2014. DuctApe: a suite for the analysis and correlation of genomic and OmniLogTM Phenotype Microarray data. *Genomics* **103**:1–10 DOI 10.1016/j.ygeno.2013.11.005.

Hastings P. 1978. Bacterial luciferase: $FMNH_2$-aldehyde oxidase. *Methods in Enzymology* **53**:558–570 DOI 10.1016/S0076-6879(78)53057-7.

Hernandez D, François P, Farinelli L, Osterås M, Schrenzel J. 2008. De novo bacterial genome sequencing: millions of very short reads assembled on a desktop computer. *Genome Research* **18**:802–809 DOI 10.1101/gr.072033.107.

Homann OR, Cai H, Becker JM, Lindquist SL. 2005. Harnessing natural diversity to probe metabolic pathways. *PLOS Genetics* **1**:e80 DOI 10.1371/journal.pgen.0010080.

Jones BW, Nishiguchi MK. 2004. Counterillumination in the Hawaiian bobtail squid, *Euprymna scolopes* Berry (Mollusca: Cephalopoda). *Marine Biology* **144**:1151–1155 DOI 10.1007/s00227-003-1285-3.

Kassem II, Splitter GA, Miller S, Rajashekara G. 2016. Let there be light! bioluminescent imaging to study bacterial pathogenesis in live animals and plants. *Advances in Biochemical Engineering/Biotechnology* **154**:119–145.

Kearse M, Moir R, Wilson A, Stones-Havas S, Cheung M, Sturrock S, Buxton S, Cooper A, Markowitz S, Duran C, Thierer T, Ashton B, Meintjes P, Drummond A. 2012. Geneious basic: an integrated and extendable desktop software platform for the organization and analysis of sequence data. *Bioinformatics* **28**:1647–1649 DOI 10.1093/bioinformatics/bts199.

Li H, Durbin R. 2010. Fast and accurate long-read alignment with Burrows-Wheeler transform. *Bioinformatics* **26**:589–595 DOI 10.1093/bioinformatics/btp698.

Li H, Handsaker B, Wysoker A, Fennell T, Ruan J, Homer N, Marth G, Abecasis G, Durbin R. 2009. The sequence alignment/map format and SAMtools. *Bioinformatics* **25**:2078–2079 DOI 10.1093/bioinformatics/btp352.

Massey S, Johnston K, Mott TM, Judy BM, Kvitko BH, Schweizer HP, Estes DM, Torres AG. 2011. *In vivo* bioluminescence imaging of *Burkholderia mallei* respiratory infection and treatment in the mouse model. *Frontiers in Microbiology* **2**:174 DOI 10.3389/fmicb.2011.00174.

Meyer-Rochow VB. 2007. Glowworms: a review of Arachnocampa spp. and kin. *Luminescence* **22**:251–265 DOI 10.1002/bio.955.

Mundy R, MacDonald TT, Dougan G, Frankel G, Wiles S. 2005. *Citrobacter rodentium* of mice and man. *Cellular Microbiology* **7**:1697–1706 DOI 10.1111/j.1462-5822.2005.00625.x.

Park S, Kim CH, Jeong WH, Lee JH, Seo SJ, Han YS, Lee IH. 2005. Effects of two hemolymph proteins on humoral defense reactions in the wax moth, *Galleria*

mellonella. *Developmental and Comparative Immunology* **29**:43–51 DOI 10.1016/j.dci.2004.06.001.

Petty NK, Bulgin R, Crepin VF, Cerdeño-Tárraga AM, Schroeder GN, Quail MA, Lennard N, Corton C, Barron A, Clark L, Toribio AL, Parkhill J, Dougan G, Frankel G, Thomson NR. 2010. The *Citrobacter rodentium* genome sequence reveals convergent evolution with human pathogenic *Escherichia coli*. *Journal of Bacteriology* **192**:525–538.

Petty NK, Feltwell T, Pickard D, Clare S, Toribio AL, Fookes M, Roberts K, Monson R, Nair S, Kingsley RA, Bulgin R, Wiles S, Goulding D, Keane T, Corton C, Lennard N, Harris D, Willey D, Rance R, Yu L, Choudhary JS, Churcher C, Quail MA, Parkhill J, Frankel G, Dougan G, Salmond GP, Thomson NR. 2011. *Citrobacter rodentium* is an unstable pathogen showing evidence of significant genomic flux. *PLoS Path*. **7**:e1002018 DOI 10.1371/journal.ppat.1002018.

Reuter S, Connor TR, Barquist L, Walker D, Feltwell T, Harris SR, Fookes M, Hall ME, Petty NK, Fuchs TM, Corander J, Dufour M, Ringwood T, Savin C, Bouchier C, Martin L, Miettinen M, Shubin M, Riehm JM, Laukkanen-Ninios R, Sihvonen LM, Siitonen A, Skurnik M, Falcão JP, Fukushima H, Scholz HC, Prentice MB, Wren BW, Parkhill J, Carniel E, Achtman M, McNally A, Thomson NR. 2014. Parallel independent evolution of pathogenicity within the genus *Yersinia*. *Proceedings of the National Academy of Sciences of the United States of America* **111**:6768–6773.

Sanz P, Teel LD, Alem F, Carvalho HM, Darnell SC, O'Brien AD. 2008. Detection of *Bacillus anthracis* sporegermination *in vivo* by bioluminescence imaging. *Infection and Immunity* **76**:1036–1047 DOI 10.1128/IAI.00985-07.

Smyth GK. 2004. Linear models and empirical bayes methods for assessing differential expression in microarray experiments. *Statistical Applications in Genetics and Molecular Biology* **3**:Article 3.

Soo VW, Hanson-Manful P, Patrick WM. 2011. Artificialgene amplification reveals an abundance of promiscuous resistance determinants in *Escherichia coli*. *Proceedings of the National Academy of Sciences of the United States of America* **108**:1484–1489.

Steinhuber A, Landmann R, Goerke C, Wolz C, Flückiger U. 2008. Bioluminescence imaging to study the promoter activity of *hla* of *Staphylococcus aureus in vitro* and *in vivo*. *International Journal of Medical Microbiology* **298**:599–605 DOI 10.1016/j.ijmm.2007.09.008.

Sun Y, Connor MG, Pennington JM, Lawrenz MB. 2012. Development of bioluminescent bioreporters for *in vitro* and *in vivo* tracking of *Yersinia pestis*. *PLoS ONE* **7**:e47123 DOI 10.1371/journal.pone.0047123.

Szittner R, Meighen E. 1990. Nucleotide sequence, expression, and properties of luciferase coded by *lux* genes from a terrestrial bacterium. *Journal of Biological Chemistry* **265**:16581–16587.

Taylor RK, Miller VL, Furlong DB, Mekalanos JJ. 1987. Use of *phoA* gene fusions to identify a pilus colonization factor coordinately regulated with cholera toxin. *Proceedings of the National Academy of Sciences of the United States of America* **84**:2833–2837 DOI 10.1073/pnas.84.9.2833.

Vencl FV. 2004. Allometry and proximate mechanisms of sexual selection in photinus fireflies, and some other beetles. *Integr. Comp. Biol.* **44**:242–249 DOI 10.1093/icb/44.3.242.

Vogel H, Altincicek B, Glöckner G, Vilcinskas A. 2011. A comprehensive transcriptome and immune-gene repertoire of the lepidopteran model host *Galleria mellonella*. *BMC Genomics* **12**:308 DOI 10.1186/1471-2164-12-308.

Wiles S, Clare S, Harker J, Huett A, Young D, Dougan G, Frankel G. 2004. Organ specificity, colonization and clearance dynamics *in vivo* following oral challenges with the murine pathogen *Citrobacter rodentium*. *Cellular Microbiology* **6**:963–972. Erratum: Cellular Microbiology **7**:459 (2005).

Wiles S, Dougan G, Frankel G. 2005. Emergence of a 'hyperinfectious' bacterial state after passage of *Citrobacter rodentium* through the host gastrointestinal tract. *Cellular Microbiology* **7**:1163–1172 DOI 10.1111/j.1462-5822.2005.00544.x.

Wiles S, Pickard KM, Peng K, MacDonald TT, Frankel G. 2006. *In vivo* bioluminescence imaging of the murine pathogen *Citrobacter rodentium*. *Infection and Immunity* **74**:5391–5396.

Winson MK, Swif TS, Hill PJ, Sims CM, Griesmayr G, Bycroft BW, Williams P, Stewart GS. 1998. Engineering the *luxCDABE* genes from *Photorhabdus luminescens* to provide a bioluminescent reporter for constitutive and promoter probe plasmids and mini-TN*5* constructs. *FEMS Microbiology Letters* **163**:193–202 DOI 10.1111/j.1574-6968.1998.tb13045.x.